

Hijack Vertical Federated Learning Models with Adversarial Embedding

Pengyu Qiu
Zhejiang University

Xuhong Zhang
Zhejiang University

Shouling Ji
Zhejiang University

Changjiang Li
Pennsylvania State University

Yuwen Pu
Zhejiang University

Xing Yang
National University of Defense Technology

Ting Wang
Pennsylvania State University

ABSTRACT

Vertical federated learning (VFL) is an emerging paradigm that enables collaborators to build machine learning models together in a distributed fashion. In general, these parties have a group of users in common but own different features. Existing VFL frameworks use cryptographic techniques to provide data privacy and security guarantees, leading to a line of works studying computing efficiency and fast implementation. However, the security of VFL's model remains underexplored.

On the other hand, recent years have witnessed the explosive growth of deep neural networks (DNNs) in industry. However, a line of works has revealed they are fragile to two attack vectors, i.e., adversarial and poisoning attacks, which aim to induce the model to give expected predictions of adversaries. Following this, a natural and interesting question is how harmful are these attacks to VFL? Our pre-study finds that existing attacks suffer from high performance degradation under VFL's mechanism. One important reason is that the multiparty collaboration mechanism weakens the adversary's influence on the final prediction results. After analyzing the challenges encountered by these attacks, we propose two new attacks, i.e., *replay attack* and *generation attack*, against VFL to reveal its potential risks of being maliciously manipulated by one participant. Specifically, the former searches for benign robust features in existing samples to determine the desired class, while the latter obtains them through adversarial generation. Furthermore, to avoid these features being suppressed by the features of other parties, we take the joint force of adversarial and poisoning attacks, i.e., implanting 'trigger-like' features in training. Finally, the adversary combines the robust features with the implanted trigger-like features to replace a target sample's features, which results in the adversary's desired prediction. Evaluation results demonstrate the effectiveness of our attacks, e.g., the adversary holding only 10% of the features can achieve an attack success rate close to 90% on a binary classifier. In addition, we evaluate potential countermeasures. Experimental results show their defense capability is limited and usually at the cost of performance loss of the VFL task. Our work highlights the need for advanced defenses to protect the prediction results of a VFL model and calls for more exploration of VFL's security issues.

1 INTRODUCTION

With data becoming a valuable resource, the discussion of illegal data collection and data leakage appears more frequently [2, 15,

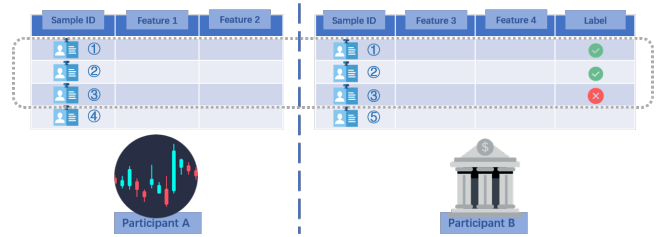


Figure 1: An example illustration of VFL. Party A is a financial company holding features 1 and 2, and party B is a bank possessing features 3 and 4. They collaborate to train a model predicting if a loan application should be approved.

27, 30, 34, 93]. These voices make the protection of personal data become a consensus. As a result, governments propose GDPR [77], CCPA[36], etc., to determine the boundaries of data collection, sharing, and transactions. These measures prevent companies from maliciously collecting personal data. On the other hand, to some extent, they also limit the ability of companies to use data for developing new businesses.

To address the dilemma, as one promising solution, federated learning (FL) [8, 13, 25, 88, 89] is an emerging paradigm that enables different data owners to build a machine learning (ML) model together. In particular, VFL handles the situation where the participants hold the same set of samples but with different features, which is different from horizontal FL (HFL) that enables the collaboration where the participants share the same feature space but have different samples. Figure 1 shows an example of VFL between a bank and a financial company. The bank and the financial company have a group of users in common, but they have different features of users. For example, the bank usually has users' savings and loan data, while the financial company has users' stocks, security information, etc. Then, when the bank wants to improve its model of evaluating a loan application, it is a natural choice for it to incorporate features from the financial company. In such scenarios, VFL has been proven effective in practice [44, 58, 82, 83, 91] and is attracting companies to invest in related applications [11, 43]. However, compared to HFL [5, 53, 57, 92], the privacy and security analysis for VFL remains underexplored.

On the other hand, despite DNNs, the most popular ML method, achieve impressive performance in many areas [1, 38, 66, 71, 74], recent works [10, 22, 33, 51, 55, 63, 68] show DNNs face several security challenges, e.g., adversarial and poisoning attacks, which aim to induce the model to give the desired output of an adversary.

Taking the case in Figure 1 for example, given a loan application which is ‘not qualified’, the adversarial attack generates a stealthy perturbation on the application to make the model predict ‘pass’; while the poisoning attack injects a trigger, usually a designed pattern, in training, and adds the trigger on the application at inference time to get the desired output ‘pass’. These manipulated misclassifications can have disastrous consequences, e.g., the collapse of the financial system due to non-performing loans [62]. Intuition is that VFL inherits these risks. However, the question is: *how harmful are these two attacks in VFL?*

In our pre-study, we find that when the adversary owns the labels (usually the initiator of a VFL model), the poisoning attack is easy to implement in VFL, and the attack success rate is consistent with the results in the centralized setting[46]. Therefore, in this paper, we do not discuss this scenario. It is a typical setting that a party in VFL only provides features [82, 83], e.g., the financial company in Figure 1 is paid to provide user information for the bank. We assume this feature-providing party is adversarial. Then, we investigate the effectiveness of the existing poisoning attack. Obviously, the ones that rely on modifying the labels of poisoning samples are not applicable, as no label information is available. Another line of work [63, 75] called clean-label attack, which relaxes the assumption to only knowing labels, is also inefficient in VFL. Specifically, the clean-label attack’s core idea is to make feature collision [63]. That is, for a target instance which is not in the training set, the clean-label attack first picks up a batch of samples from the desired class and then adds invisible perturbations to these samples to make their latent embeddings close to that of the target instance. Then, when the target instance is being inferred, it will be misclassified as the desired class. Since multiple parties in VFL determine a sample’s latent embedding, it is hard for the adversary to make feature collision with partial control of the embedding. Additionally, it also means the adversary might need to poison much more samples in VFL than that in the centralized setting.

As for the adversarial attacks, since the adversary only has a part of the VFL model, a line of work with the white-box assumption, e.g., the complete access to the model, is not applicable. Then, for the black-box attacks, the partial control of the features also limits their performance. Specifically, in the centralized setting, the query-based attacks [12, 28, 70] are able to achieve impressive performance with limited pixels [9], even one pixel [67]. The success of these attacks is based on the assumption that the adversary can find out the most important pixels through queries and modify their values to change the prediction results. Unfortunately, in VFL, an adversary can only modify his/her features. When the adversary’s features are not given enough importance, e.g., small activation values, the adversarial attack fails. In addition, if the adversary’s feature importance is not dominant, he/she may also need additional queries to strengthen the adversarial perturbation’s effect.

From the above analysis, we find that the partial control of the features limits the application of both poisoning attacks and adversarial attacks, and the cost of attacking a single instance in VFL is usually much more huge. Then, a challenging research question is: *can we implement a new efficient attack in VFL? Specifically, an attack that works on a class of samples and assumes only limited knowledge, e.g., a small set of labels or a small number of queries?* To address

the above challenge, in this paper, we propose two attacks, *replay attack* and *generation attack*, to reveal the VFL model’s potential risks of being maliciously manipulated by a participant.

The replay attack, which is simple yet effective, is based on the intuition that benign robust features can also trigger feature collision. Specifically, the adversary first selects samples that have high confidence in the target class and stores their features. Then, for a target sample, the adversary replaces its features at his/her side with the selected features to make the prediction flipped (e.g., ‘not qualified’ to ‘pass’ of a loan application in Figure 1). Compared to the clean-label attack, our replay attack makes the robust features reusable. However, a disadvantage of this attack is that it can only search for existing features, which may not be optimal. Therefore, we further propose the generation attack, which turns the searching process into an optimization problem. The purpose of the generation attack is searching for the optimal robust features, even if these features might not exist in the training samples. The optimal features are similar to the concept of the centroid in k-means clustering[50]. Different from the adversarial attack, our generation attack also aims to make the generated features reusable.

Ideally, the features collected by both attacks are supposed to determine a class of samples’ prediction result regardless of the features provided by other participants. However, the above attack designs still face the challenge that the adversary only controls a few features when multiple parties participate in VFL. The adversary’s influence on the final prediction might be limited in this situation. Therefore, we further combine a poisoning phase with our proposed attacks to solve the dilemma. The poisoning phase, however, is not used to inject a trigger to flip the prediction results like traditional poisoning attacks. Its purpose is to attract the VFL model’s attention to the adversary’s features. Specifically, by implanting a ‘trigger-like’ feature frequently in the samples of the target class, it is easier to make the VFL model learn the connection of the feature and the class [76], and thus gives the adversary’s features sufficient importance in the prediction of the target class.

In addition, we investigate the scene where the adversary cannot access the outputs of the VFL model, which is a more stringent scenario for the adversary. We find that our attacks can still work with a small portion of auxiliary samples. Specifically, we use mix-up [90], which is used for training an ML model with a limited number of samples, for obtaining a surrogate model. Unlike the surrogate models in adversarial attacks used for generating transferable adversarial perturbations, this one is used to select features that may determine the target class only with the adversary’s features. In Section 2.4, we detail the threat model, in which we characterize the adversary’s background knowledge along two dimensions: the access to the VFL model’s prediction results and the auxiliary dataset with a small portion of ground truth labels.

We evaluate our attacks under different scenarios in Section 5. The experimental results show that our attacks combined with the poisoning attack can achieve impressive performance, e.g., the adversary holding only 10% of the features can achieve an attack success rate close to 90% on a binary classifier. We evaluate two possible countermeasures in light of these attacks, i.e., input transformation and dropout. The results show that these defenses’ effect is limited and bear the cost of performance loss of the VFL task.

Our contributions can be summarized as follows.

- To the best of our knowledge, we are the first work to investigate the malicious usage of robust features in VFL.
- We propose two specific attack methods and their variants according to the adversary’s background knowledge. These attacks are convenient to initiate and can achieve a high attack success rate even if the adversary is the weaker party in VFL.
- We conduct extensive evaluations on real-world datasets, including tabular, image, text, and multi-modal data types. The results demonstrate the effectiveness of our attacks.
- We also analyze existing defenses and apply two selected solutions to defend against our attacks. However, experimental results show that their defense effect is limited, highlighting the need to design advanced defense mechanisms to mitigate the malicious target attack.

2 PRELIMINARIES

We begin by introducing a set of fundamental concepts and assumptions. Table 2 (defer to Appendix A due to the page limitation) summarizes the important notations in the paper.

2.1 Deep Neural Networks

Deep neural network (DNN) is the most popular machine learning method in recent decades, exhibiting powerful feature extraction ability. Specifically, a DNN f with parameters θ represents a function $f : \mathcal{X} \rightarrow \mathcal{Y}$, where \mathcal{X} denotes the input space and \mathcal{Y} denotes the pre-defined classes.

Take a classification task for example. Given a training set D , of which each instance $(x, y) \in D \subset \mathcal{X} \times \mathcal{Y}$ consists of an input x and its label y . A DNN f is trained to find the best parameters θ by minimizing the loss function ℓ (usually cross entropy loss for classification tasks). Formally, the search for the best θ can be formulated as the optimization objective:

$$\min_{\theta} \mathbb{E}_{(x,y) \in D} [\ell(x, y; \theta)],$$

where $\mathbb{E}[\cdot]$ denotes the expected loss of $f(x; \theta)$ and y of D .

2.2 Attack Vectors against DNNs

Recently, a line of works focuses on exploring the vulnerability of DNNs, whose goal is to induce the model to give expected prediction results of adversaries. In general, these works can be categorized into two primary attack vectors, namely, adversarial attacks and poisoning attacks, where the former is an inference phase attack, and the latter is a training phase attack. Below, we introduce them in a detailed manner.

2.2.1 Adversarial Attack. Under this attack, an adversary crafts an adversarial perturbation of a sample to fool the target DNN at the inference phase. For example, in image classification, given an input image, x , e.g., ‘cat’, and the target DNN model f , the adversary can change f ’s prediction from ‘cat’ to whatever he/she desires, e.g., ‘dog’, with a generated perturbation δ imposed on x . To make the attack stealthy, the adversary often restricts δ within a small range, e.g., a norm ball at the original point, $\mathcal{B}_{\epsilon}(0) = \{\delta \mid \|\delta - 0\|_p \leq \epsilon\}$, where p denotes the L_p norm and ϵ denotes the bound. Formally, the generation of such a perturbation is formulated as the optimization

objective:

$$\delta_* = \arg \min_{\delta \in \mathcal{B}_{\epsilon}(0)} \ell(\delta + x, t; \theta) \quad (1)$$

where ℓ measures the loss of the perturbed sample’s prediction with the target class t ; θ is the parameters of f .

Many works have studied the optimization of Eq 1. According to the adversary’s knowledge about θ , there are two primary categories: white-box and black-box attacks. In the white-box scenario, the adversary knows the model’s structure and parameters. Therefore, the perturbation can be optimized by the gradient descent method, such as FGSM[22], PGD [51], and C&W [10]. In the black-box scenario, the adversary only has access to the model’s output, which means he/she cannot obtain the gradients. To address this, there are two streams for approximating the gradients. One class is the differential method [12], which calculates the perturbation’s gradients through the difference of two queries. The other class tries to approximate the gradients by a surrogate model [41], which is trained on an auxiliary dataset that is independently and identically distributed (i.i.d) to the training dataset.

2.2.2 Poisoning Attack. Under this attack, the adversary aims to pollute DNNs during the training phase. Previous works [3, 31, 86] focus on decreasing the model’s utility, e.g., making the model unable to converge in training by modifying the training data. Recently, a line of works [5, 32, 63] finds that by adding a fixed pattern, e.g., a square patch on an image, on poisoning samples, they can induce the model to give desired predictions whenever it meets the pattern. This pattern is also called a backdoor trigger. In the following, we also refer to the poisoning attacks as backdoor attacks, as they better meet the purpose of our attacks.

Poisoning attacks can be formulated as perturbing the model’s parameters θ , and we denote the perturbed parameters by θ_{δ} . To ensure the evasiveness of the attack, the adversary also limits the perturbation on θ in a given function space \mathcal{F} . We define the search space as $\mathcal{F}_{\epsilon}(\theta) = \{\theta_{\delta} \mid \mathbb{E}_{x \in D_{val}} [|f(x; \theta_{\delta}) - f(x; \theta)|] \leq \epsilon\}$, where D_{val} refers to the validation dataset. According to the formula, θ_{δ} should maintain the inference performance for benign samples. Formally, we give the formulated definition as the following optimization function:

$$\theta_* = \arg \min_{\theta_{\delta} \in \mathcal{F}_{\epsilon}(\theta)} \mathbb{E}_{x \in D_{target}} [\ell(x, t; \theta_{\delta})] \quad (2)$$

where D_{target} denotes the set of inputs containing the trigger, and the loss function is defined similarly to Eq 1.

In practice, the optimization for Eq 2 is difficult. Therefore, many works focus on polluting the training data [32, 63] and modifying DNNs [72]. In the former kind of attacks, the adversary limits the perturbation to θ by reducing the number of polluted samples or improving the trigger’s signal to the model. While in the latter kind of attacks, the adversary modifies the neurons or adds extra structures in the DNN.

2.2.3 Clean-label Attack. Since the clean-label attack [63], like our work, assumes that the adversary cannot modify the labels, we briefly describe their method in this section.

The authors believed that an adversary could not control the labeling process, and even if he/she does, the mislabelled samples are easy to recognize [63]. Therefore, they proposed a more stealthy

method via feature collision. That is, the adversary first picks up a sample from the desired class, e.g., an image of ‘cat’, and then adds an invisible perturbation to it. The perturbation is used to make this poisoned sample’s latent embedding as close to that of the target instance (e.g., an image of ‘dog’) as possible. Then, when the target instance is being inferred, it will be misclassified as ‘cat’.

Formally, let f be the model without the last softmax layer, x be the sample from the desired class, and t be the target sample. A poisoning sample p is crafted as follows:

$$p = \arg \min_p \|f(p) - f(t)\|_2^2 + \beta \|p - x\|_2^2 \quad (3)$$

where β is a hyperparameter that controls the similarity between the poison sample p and original sample x . Usually, the clean-label attack needs a number of poisoning samples for one target instance.

2.3 Vertical Federated Learning

Consider a classification task and a set of m distributed parties $\{P_1, P_2, \dots, P_m\}$ with datasets $\{D_1, D_2, \dots, D_m\}$. For each dataset, $D_i = (U_i, F_i)$, where U_i denotes the sample space and F_i denotes the feature space. Before training, VFL needs to first determine the sample space U , which is $U = \bigcap_{i=1}^m U_i$. Then for features from different F_i , VFL aligns them for each sample.

After the preparation of data, P_i trains its bottom model, denoted by f_i , to extract the high-level abstractions of each sample. Let x_i^u denote the feature vector of sample u with d_i features from F_i . Then the function of f_i is to map the feature vector to a d^* -dimensional latent space, i.e., $f_i(x_i^u; \theta_i) : \mathbb{R}^{d_i} \rightarrow \mathbb{R}^{d^*}$. θ_i denotes the parameters of f_i and is optimized by a specific objective function. We use v_i^u to represent the output of f_i . For simplicity, unless otherwise defined, we use v_i instead of v_i^u in the following.

After each participant uploads v_i to a neutral third party server (NTS), they are concatenated for further calculations. Specifically, let $v_{cat} = [v_1, v_2, \dots, v_m]$ and f_{top} denote the top model located at NTS. f_{top} learns a mapping from v_{cat} to v_{top} , i.e., $f_{top}(v_{cat}; \theta_{top}) : \mathbb{R}^{m \times d^*} \rightarrow \mathbb{R}^{n_c}$, where n_c denotes the number of classes, and v_{top} is the output of f_{top} , which is also the posterior of a sample. Finally, v_{top} is sent to the party who owns the labels to calculate the loss, e.g., cross-entropy loss. The loss is then used to optimize each model’s parameters, including f_{top} and f_i . Formally, the training of VFL is formulated as follows:

$$\min_{\{\theta_i\}_{i=1}^{m+1}} \mathbb{E}_{u \in U} [\ell(x_1, x_2, \dots, x_m, c; \{\theta_i\}_{i=1}^{m+1})]$$

where ℓ refers to the loss function; c is the label of the sample u ; and we use θ_{m+1} to represent θ_{top} .

2.4 Threat Model

2.4.1 Adversary. We assume the adversary is a malicious participant of VFL who only provides features. He/she controls the bottom model and can arbitrarily modify its output.

2.4.2 Adversary’s Goal. The adversary’s goal is to make the VFL model predict a set of target samples as the adversary-chosen target class. In this paper, the set of target samples come from the adversary-chosen source class. The adversary’s purpose might be earning profits by providing a service that modifies the results of a user’s loan application at a bank.

2.4.3 Adversary’s Knowledge. We characterize the adversary’s background knowledge along two dimensions.

- **Access to the posteriors, denoted by \mathcal{P} .** The knowledge of \mathcal{P} is reasonable for the adversary to know in practice since the interpretability of the prediction is important for each party in making further decisions [47, 84]. For example, the posteriors can provide the details of the probability distribution across different classes, while the hard labels cannot. Moreover, according to [79], \mathcal{P} is also essential to data valuation in VFL, which determines the profit of each participant. Therefore, the adversary still has the chance to obtain this knowledge.
- **Auxiliary dataset, denoted by \mathcal{L} .** This knowledge means that the adversary has a small portion of label information, e.g., 1% of the number of the target class in a dataset, in addition to his/her features. However, he/she cannot modify any samples’ labels.

We further divide this knowledge into two categories, \mathcal{L}_{target} and \mathcal{L}_{all} . \mathcal{L}_{target} refers to a set of samples belonging to the target class t ; while \mathcal{L}_{all} represents the auxiliary dataset that has samples from all the classes. Furthermore, the samples belonging to the target class in \mathcal{L}_{all} and those in \mathcal{L}_{target} should also exist in other participants. Thus we can carry out the poisoning attack.

The assumption of \mathcal{L} is not difficult to satisfy. As a participant of VFL, the adversary can first collect a small portion of candidate samples but with their labels unknown. Then he/she can obtain the ground truth labels through investigation or indirect inference. For instance, if the adversary is the financial institution interested in a user’s credit rating, it can employ a group of users to register accounts in the target bank before training and then obtain their labels [16].

Let \mathcal{K} denote the background knowledge. Then we can formally present the adversary’s knowledge as a tuple $\mathcal{K} = (\mathcal{P}, \mathcal{L})$. If one knowledge is unavailable, we denote it by \times . Then we can get six different combinations of \mathcal{K} (two choices for \mathcal{P} and three for \mathcal{L}).

However, when $\mathcal{K} = (\times, \times)$, the adversary is not able to conduct either of the two attacks. Therefore, we do not consider this case in this paper. Then, for $\mathcal{K} = (\times, \mathcal{L}_{all})$ and $\mathcal{K} = (\times, \mathcal{L}_{target})$, since \mathcal{L}_{all} contains \mathcal{L}_{target} , we merge these two kinds of knowledge together and present it by $\mathcal{K} = (\times, \mathcal{L}_{all})$. For $\mathcal{K} = (\mathcal{P}, \mathcal{L}_{all})$ and $\mathcal{K} = (\mathcal{P}, \mathcal{L}_{target})$, we exclude the case $\mathcal{K} = (\mathcal{P}, \mathcal{L}_{all})$ because \mathcal{L}_{target} is sufficient for the poisoning attack.

Finally, we get three kinds of \mathcal{K} , i.e., $\mathcal{K} = (\mathcal{P}, \times)$, $\mathcal{K} = (\mathcal{P}, \mathcal{L}_{target})$, and $\mathcal{K} = (\times, \mathcal{L}_{all})$. In Section 3, we give the detailed attack design and implementations for each of them.

3 METHODOLOGY

3.1 Overview of Attack Pipeline

Figure 2 shows the pipeline of our attacks, which can be divided into two phases: the poisoning phase and the adversarial embedding generation phase. The adversarial embedding is the output of the adversary’s model. Therefore, in the following, we do not distinguish between the adversary’s robust features and the corresponding adversarial embedding. Furthermore, in this paper, we mainly operate on the adversarial embedding instead of the raw features as the embeddings are continuous.

First, when the adversary’s knowledge \mathcal{K} contains \mathcal{L}_{target} , he/she performs the poisoning attack in the training phase. Specifically,

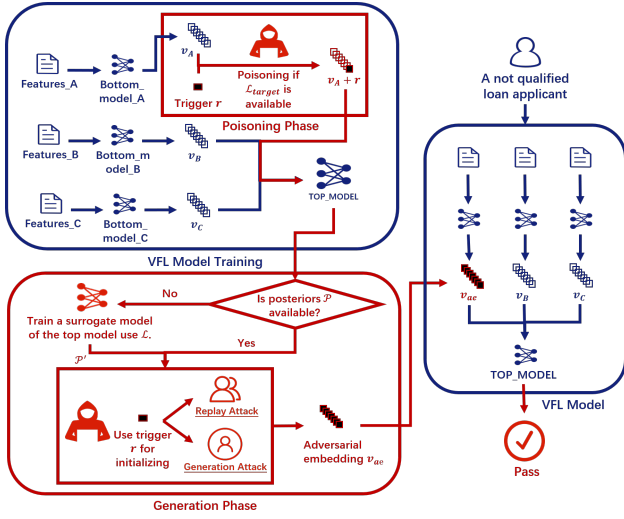


Figure 2: The overview of the attack pipeline.

the adversary generates a random Gaussian noise r and adds it on v_{adv} of each sample in \mathcal{L}_{target} . This phase aims to make the top model rely on the adversary’s features.

After training a VFL model, the adversary starts the second phase of the attack. The first step is to check whether the knowledge \mathcal{P} is accessible. If not, the adversary should train a surrogate model using \mathcal{L}_{all} . Then he/she uses the output of the surrogate model, denoted by \mathcal{P}' , to approximate \mathcal{P} . \mathcal{P} is used for the preparation of adversarial embeddings v_{ae} through two ways, i.e., replay attack and generation attack. Furthermore, the trigger r is also used in both attacks if the poisoning attack has been conducted. Specifically, the replay attack uses \mathcal{P} to find samples that have high confidence of the target class. The trigger r , if available, will be added to a candidate sample’s embedding in the selection process. As for the generation attack, we use \mathcal{P} to guide the direction of generation. We use trigger r for initialization to improve the efficiency of the generation process. For different \mathcal{K} , there are different implementations of the generation attack, which we will present in the following sections.

Finally, for a target sample, the adversary directly replaces v_{adv} with v_{ae} to get the desired prediction.

3.2 Adversary’s Knowledge: $\mathcal{K} = (\mathcal{P}, \times)$

This knowledge refers to the case where the adversary behaves honestly in training but tries to manipulate the model’s prediction at the inference phase. Formally, the generation attack under this knowledge can be formulated as the optimization function:

$$v_{ae} = \arg \min_{\delta \in \mathbb{R}^{d_s}} \ell([v_1, \dots, \delta, \dots, v_m], t; \{\theta_i\}_{i=1}^{m+1}), \quad (4)$$

where ℓ measures the entropy loss of the perturbed prediction results and the target class t , and $\{\theta_i\}_{i=1}^{m+1}$ are the models’ parameters.

The challenge of optimizing the objective function is that both $\{v_i\}_{i \neq adv}$ and $\{\theta_i\}_{i \neq adv}$ are not accessible, which means the gradients used for optimization cannot be calculated. Therefore, we use the zeroth order optimization (ZOO) method to approximate the gradients, which follows Chen et al. in [12]. Due to the page limitation, we put the details of derivation in Appendix B.

In addition, considering that in real-world applications, e.g., a loan application, a user may only apply once in a period of time. Therefore, v_{ae} should be prepared beforehand and be able to affect a set of samples. However, it is hard to generate a universal adversarial embedding without the true gradients and the control of all features. Therefore, we aim to make v_{ae} capable of changing the model’s predictions of samples belonging to a source class s . Specifically, to achieve this goal, we collect a small set of samples of s with high confidence and then optimize the objective function iteratively with them to find the best v_{ae} .

Algorithm 1 summarizes the process of the attack. First, the adversary prepares a set of samples of the source class, denoted by \mathcal{S} . Then he/she initializes δ as 0. We do not randomly initialize it because the random vector may already belong to a class. Therefore, to diminish the impact of randomness, we choose to start at 0. Then, the adversary repeats the optimization process according to the loss function for each sample s in \mathcal{S} . The loss function ℓ measures the cross entropy loss of the modified sample’s prediction result and the target class. Finally, δ is stored as v_{ae} for attack.

Algorithm 1 Class-specific Adversarial Embedding Generation

Require: Samples who have high confidence of the source class \mathcal{S} ; query budget Q .

Ensure: Adversarial embedding v_{ae} .

```

1:  $\delta \leftarrow 0, queries \leftarrow 0$ 
2: for  $s \in \mathcal{S}$  do
3:   while  $queries < \frac{Q}{|\mathcal{S}|}$  do
4:     randomly choose coordinate  $i$ 
5:      $\hat{g}_i \leftarrow \text{ZOO-Adam}(\ell([v_1, \dots, \delta, \dots, v_m]^s, t))$ 
6:      $\delta_i \leftarrow \delta_i - \hat{g}_i$ 
7:      $queries \leftarrow queries + 2$ 
8:   end while
9:    $queries \leftarrow 0$ 
10: end for
11:  $v_{ae} \leftarrow \delta$ 

```

3.3 Adversary’s Knowledge: $\mathcal{K} = (\mathcal{P}, \mathcal{L}_{target})$

When the adversary has a few features, his/her contribution to the final prediction is limited [79], as θ_{top} gives a small weight on v_{adv} . This limits the adversary’s capability and may cause that no matter how well v_{ae} is optimized, it is hard to flip the prediction. Therefore, with the help of \mathcal{L}_{target} , we design an active way to adjust the weight, i.e., perturbing θ_{top} at the training phase.

The traditional poisoning attack usually needs to modify labels for poisoning. In this paper, we assume the adversary is only a feature provider, which limits his/her ability to perform such an attack. Moreover, the adversary also cannot modify the top model’s structure. Due to these limitations, we choose to implant ‘trigger-like’ features and thereby perturb θ_{top} . Specifically, we first generate a random Gaussian noise r , and then for each sample from \mathcal{L}_{target} , we add r on its v_{adv} . Different from the goal of the clean-label attack, which aims to make a feature collision, our purpose is to induce the top model to memorize the connection between the noise r and the target class t .

Given the poisoned VFL model, the remaining procedure is similar to the previous case. The only difference is that we initialize δ

as r instead of 0. The reason is that searching in the neighborhood of r can improve the generation efficiency, as the top model may be sensitive to r . Then, the objective function is changed to:

$$v_{ae} = \arg \min_{\delta \in \mathbb{R}^{d_s}} \ell([v_1, \dots, \delta, \dots, v_m], t; \{\theta_i^*\}_{i=1}^{m+1}), \quad (5)$$

where $\{\theta_i^*\}_{i=1}^{m+1}$ are the perturbed parameters.

Algorithm 2 summarizes the process of the attack. Due to the page limitation, we put it in Appendix D.1.

3.4 Adversary’s Knowledge: $\mathcal{K} = (\times, \mathcal{L}_{all})$

In this scenario, the adversary’s knowledge is limited to the auxiliary dataset \mathcal{L}_{all} . The adversary’s role, in this case, is a participant who is paid to provide features and does not have access to the ‘feedback’ from the VFL model.

Since \mathcal{L}_{all} contains \mathcal{L}_{target} , we still let the adversary perturb the top model in training following the poisoning method in the previous section. Then, to solve the challenge of lacking \mathcal{P} , we use \mathcal{L}_{all} to train a surrogate model f_s . Specifically, the input of f_s is v_{adv} (+ r if the sample belongs to the target class). The purpose is to let f_s approximate the classification boundary of f_{top} only with the adversary’s features. Furthermore, to train a high-quality surrogate model with a small number of samples, we use mix-up, which is proposed by Zhang et al. in [90].

However, since f_s loses a lot of information, i.e., $\{v_i\}_{i \neq adv}$, the transferability between f_s and f_{top} is weak. Therefore, instead of generating a customized adversarial embedding for each sample, we choose to generate a universal v_{ae} and strengthen its signal related to the target class. Furthermore, since random initialization may introduce noise, we use the v_{ae} obtained via the replay attack as the initial point. Then, we perturb it to maximize the confidence of the target class calculated by the surrogate model. Formally, the attack can be formulated as the objective function:

$$v_{ae} = \arg \min_{\delta \in \mathbb{R}^{d_s}} \ell(f_s(\delta), t). \quad (6)$$

Algorithm 3 summarizes the process of the attack. Due to the page limitation, we put it in Appendix D.2.

4 EXPERIMENTAL SETUP

4.1 Datasets

We evaluate the attack performance on five public datasets, including tabular, image, text, and multi-modal data types: 1) Company Bankruptcy Prediction Dataset (denoted by BANK) [42], which was collected from the Taiwan Economic Journal for the years 1999 to 2009, consisting of 6,819 instances with 95 attributes and two classes; 2) CIFAR10 [37], which consists of 60,000 images with 10 classes; 3) CIFAR100 [37], which expands the classes to 100 compared to CIFAR10; 4) IMDB [49], which contains 50,000 movie reviews with two classes; and 5) Android Permission Dataset (denoted by AP) [52], which contains 20,000 android APPs’ permission statistics and descriptions with two classes.

For BANK and AP, we further use the oversampling method to balance the number of samples in each category. Then we split the training and testing data with a ratio of 7:3. As for CIFAR10, CIFAR100, and IMDB, we adopt their default settings. Specifically, CIFAR10 uses 50,000 images in the training and 10,000 images for

testing, so as for CIFAR100. IMDB, however, uses 25,000 reviews in training and 25,000 reviews for testing.

4.2 Models

We train the VFL model in a local environment and mark one bottom model as the adversary’s model. Specifically, the top model is composed of dense layers, i.e., an input layer, an output layer, and one hidden layer. The bottom model, however, is chosen by the modal of data. For tabular data, we use DNNs composed of three dense layers to calculate embeddings. Then, for image data, we use ResNet [26] instead. Furthermore, for text data, we use BERT [14] as the bottom model. The surrogate model is composed of one fully connected layer. Table 3, deferred to Appendix C.1 due to the space limitation, summarizes the details of the used models.

4.3 Metric

We evaluate the attack performance with the attack success rate (ASR), which is defined as follows:

$$\frac{\sum_{u \in \mathcal{D}_{test}} I(\arg \max(f(v_1^u, \dots, v_m^u; \theta_{top})) = t)}{\|\mathcal{D}_{test}\|}$$

where $I(\cdot)$ is an indicator function and \mathcal{D}_{test} denotes the testing dataset.

For both the replay attack and the generation attack, the phase for generating the adversarial embedding is repeated 10 times. We use the one with the highest ASR in our evaluation. It is because we can test the performance of our attacks on a set of samples for validation. These samples can be collected from the auxiliary dataset \mathcal{L}_{all} or in the final round of training, where we use their posteriors as ground truth labels. Then, it is reasonable to abandon v_{ae} that does not perform well.

4.4 Implementation

Following [16, 47], we consider the most popular two-party VFL as our primary case and further analyze the impact of the number of parties in Section 6. This setting is reasonable, as in industry, the intersection of samples will decrease rapidly with the number of companies increasing. Furthermore, the computation and communication cost of the multi-party case is also a realistic consideration for companies. Therefore, two-party VFL is now the most popular scenario in the real world [48]. Nevertheless, to evaluate the generalization of our attacks in a multi-party scenario, we also conduct the corresponding experiments in Section 6.1.

We limit our generation attack with the query budget of 300 times, which is comparable to the number in [12]. Table 4, deferred to Appendix C.2 due to the space limitation, summarizes other default settings.

4.5 Environment

We implement the attacks in Python and conduct all experiments on a workstation equipped with AMD Ryzen 9 3950X and an NVIDIA GTX 3090 GPU card. We use PyTorch to implement the models used in the experiments, and pandas and sklearn for data preprocess.

5 EVALUATION

In this section, we consider three evaluation scenarios according to \mathcal{K} . Specifically, in Section 5.1, when $\mathcal{K} = (\mathcal{P}, \times)$, we answer the question of how effective our attacks are in the basic setting. Then, in Section 5.2, the experiments are conducted to evaluate the advantages of combining the poisoning attack. Finally, in Section 5.3, which is the most strict setting, we evaluate whether the samples with a strong perturbing signal could still be found or generated.

In addition, since the adversarial embedding generated via \mathcal{P} focuses on changing the predictions of samples belonging to the source class, the following evaluations and comparisons are also based on a fixed source class. Specifically, we refer to ‘0’ as the source class, which is ‘bankrupt’ in BANK, ‘airplane’ in CIFAR10, ‘apple’ in CIFAR100, ‘negative’ in IMDB, and ‘benign’ in AP. Then, the target class is ‘1’ for binary classification tasks, e.g., BANK, IMDB, and AP. For CIFAR10 and CIFAR100, we also fix the target class as ‘1’ (automobile and aquarium fish, respectively) to keep the consistency. The impact of the source class is analyzed in Section 6.3.

5.1 Attack with Posteriors

In this section, we evaluate our attacks with $\mathcal{K} = (\mathcal{P}, \times)$. Specifically, we answer the following questions.

- How effective is replay attack in a normal VFL model?
- Is the adversarial embedding capable of changing the model’s predictions from a source class to a target class?
- Do our attacks work across all types of datasets?

We first introduce the configuration of datasets and then give the details of the results.

Dataset Configuration To construct the two-party VFL, we follow the practice in [46] and split the features into two parts. We vary the feature ratio of the adversary from 10% to 90% to approximate the adversary’s feature importance to the VFL model, where the feature ratio represents the portion of features owned by the adversary. According to the conclusions in [79], Guan et al. pointed out that, in VFL, the party’s contribution to the prediction results is proportional to the number of features he/she has.

In general, the participant who owns the labels has more features. However, there are also cases where the participant only provides labels but no features [83]. For example, in Figure 1, if the financial institution wants to build a risk management system since only the bank can have personal credit information according to local laws, it should possess all the related features for the task.

We use three kinds of datasets in our evaluation, i.e., tabular, image and text. For tabular data, it is easy to split it into two parts. Then for images, we split them vertically. For example, if the feature ratio is 50%, we split an image from the center. As for texts, we split them by the portion of words.

Attack Performance Figure 3 plots the results of our attacks. First of all, for BANK and CIFAR10, the replay attack reaches a high ASR when the feature ratio is higher than 50% but almost fails with low feature ratios. It is natural since the adversary’s contribution to the top model is limited when he/she has a few features. For IMDB, however, the attack achieves an ASR of nearly 100% at almost all feature ratios, except for the feature ratio of 50%. We speculate that this is because, for a movie review, the

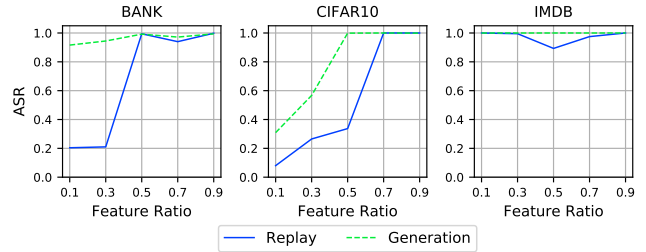


Figure 3: Attack performance with posteriors. The x-axis represents the ratio of features the adversary has. The y-axis represents the ASR of our attacks.

first sentence mostly represents the reviewer’s attitude. Therefore, although the adversary has a few features, he/she can still flip the predictions with words having strong emotions.

The exception, however, also exists in BANK. As the feature ratio increases, the ASR first drops a little, then rises again, e.g., when the feature ratio is 70% for BANK and 50% for IMDB. We speculate that the noise of features causes this. Indeed, we find that the selected samples in the replay attack are different with different feature ratios. That means a sample may have a strong signal at the feature ratio of 50%, but its signal decreases when the ratio is 70%. This is reasonable because a sample’s different features will not always point to one class, as a person’s record in the bank will not always be good.

As for the generation attack, it is quite impressive on the three datasets. For example, for BANK and IMDB, we achieve an ASR of over 90% when the feature ratio is only 10%. For CIFAR10, the highest ASR is 100% when the feature ratio is over 50%. However, its ASR is 38% at the ratio of 10% and 60% at the ratio of 30%. We speculate that the performance difference between CIFAR10 and the other two datasets at the low feature ratio is caused by the number of classes. Indeed, with more classes, the model will produce a much more complex classification boundary. Therefore, finding the best optimization path with a tight budget is not easy (the number of queries for optimization). In Section 6.2, we further investigate the impact of the number of classes on our attacks, and the experimental results confirm our speculation.

The above results prove that the success of our attacks is independent of the type of datasets. It is expected since our attacks focus on the embedding extracted by the bottom model. The performance difference between different data types is that for tabular and text, an attribute or a word may be decisive; however, for an image, it requires a salient object, e.g., cat ears.

5.2 Attack with Posteriors and Auxiliary Samples

In this section, we have the most knowledge and can perform both the poisoning attack and the adversarial attack. Our experiments are to verify our speculations as follows.

- The poisoning attack alone cannot work with a limited number of poisoning samples;
- The perturbed model will adjust its weight, leading to a better performance of replay attack and generation attack;
- Searching from the neighborhood of trigger can improve the efficiency.

Accordingly, we evaluate five kinds of attacks in this section: poisoning attack, replay attack, replay attack with trigger, generation attack, and generation attack with trigger.

The poisoning attack is trivial, of which we add the trigger on v_{adv} at the inference time to see the ASR. Compared to the replay attack, the replay attack with trigger denotes the attack in which we further add the trigger on samples' v_{adv} during the selection process. Similarly, the difference between the generation attack and the generation attack with trigger is that the former starts at the origin point, while the latter starts at the trigger point.

Dataset Configuration The training dataset and testing dataset are the same as that in Section 5.1. As for the auxiliary samples, we randomly sample them from the training dataset. Specifically, we keep the sample rate at 1%, e.g., for CIFAR10, we only sample 50 images of the target class for the poisoning attack. Compared to existing poisoning attack settings [63], our setting is pretty strict for the adversary.

Attack Performance Figure 4 shows the results of our attacks. In general, our attack using both attack vectors shows a powerful capability of manipulating the top model's output. For BANK, our generation attack with trigger achieves an ASR of 98% at the feature ratio of 10%. Even with CIFAR10, it reaches an ASR of over 56%, almost twice the ASR in the previous scenario. Furthermore, when the feature ratio is over 30%, the ASR is all over 90% on each dataset, which implies a severe vulnerability of VFL. This result shows that even if a participant is only a feature provider, it can maliciously manipulate the final result through our integrated attack.

The poisoning attack, which only uses the trigger, cannot achieve a high ASR on the three datasets. We speculate that the restriction of modifying labels and the number of poisoned samples limit its efficiency. However, we would like to mention that our goal of using the poisoning attack is to make the top model rely more on the adversarial party rather than performing the usual high-performance poisoning attack. Both our generation attack and replay attack benefit from the poisoning attack compared to the results in the previous case. For example, for CIFAR10, when the feature ratio is 30%, the performance of the generation attack is improved from 60% to 92% with the help of the poisoning attack. Similarly, the replay attack's performance is improved from 32% to 63% when the ratio is 50%. Furthermore, the comparison between the generation attack with and without trigger shows that searching from the trigger's neighborhood can achieve a better ASR, demonstrated by the performance gap at the feature ratio of 10% on CIFAR10.

In addition, the drop of ASR for BANK at the feature ratio of 70% still exists and is amplified by the poison attack. The reason is the same as we analyzed in Section 5.1.

5.3 Attack with Auxiliary Dataset

In this section, we evaluate our attack's performance when \mathcal{K} is restricted to \mathcal{L}_{all} . Specifically, the experiments are conducted to explore whether we can still find or generate embeddings with strong signals related to the target class.

Dataset Configuration The auxiliary dataset is also sampled from the training dataset, and the sampling ratio is still 1%. For CIFAR10, this means we only have 500 images in total and 50 for

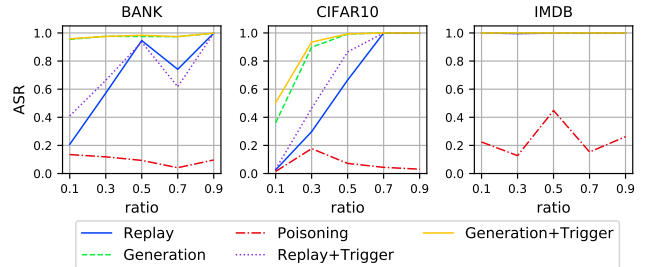


Figure 4: Attack performance with posteriors and auxiliary samples of the target class. The x-axis represents the ratio of features possessed by the adversary. The y-axis represents the ASR of our attacks.

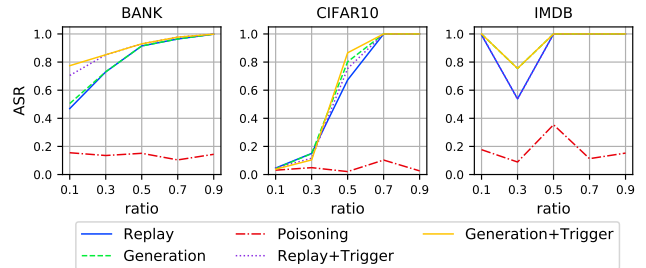


Figure 5: Attack performance with auxiliary dataset. The x-axis represents the ratio of features the adversary has. The y-axis represents the ASR of our attacks.

each class. This is also a challenging setup for training our mix-up based surrogate model.

Attack Performance Figure 5 shows the results of our attacks. Compared to the previous two scenarios, the performance of our generation attacks, including with/without trigger, drops. This phenomenon is expected since we have no global information to optimize the adversarial embedding but focus on maximizing the confidence given by the surrogate model. Therefore, the information loss brought by the surrogate model and the potential overfitting of the embedding on the surrogate model cause the decrease of performance together. However, they are still powerful when the feature ratio is over 50%. For BANK, the generation attack with trigger can even achieve an ASR of 79% at the ratio of 10%.

In addition, under this scenario, our integrated attack still performs better than others, verifying that perturbing the model's parameters and preparing the adversarial embedding are both necessary for changing the model's predictions.

6 SENSITIVITY ANALYSIS

In this section, we further evaluate the impact of the default setting in the previous experiments. Specifically, we answer several research questions as follows.

- How does the number of parties affect our attacks?
- Will more classes invalidate our attacks?
- Will different source classes affect our attacks?

6.1 Number of Parties

In this section, we evaluate the impact of the number of parties on our attacks. We fix the adversary's feature ratio at 10%, and for each

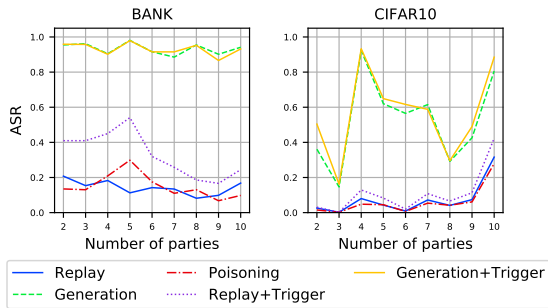


Figure 6: Attack performance with different number of parties. The x-axis represents the number of parties. The y-axis represents the ASR of our attacks.

newly added participant, we will assign it 10% of the total features. For example, when the number of participants is 3, the ratio of features of both the adversary and the newly joined participants is 10%, and the participant with labels owns the remaining 80%. When there are 10 participants, each one has 10% of the features. We use BANK and CIFAR10 in this evaluation. In the previous evaluation, the results on IMDB do not show apparent sensitivity of feature ratios. Therefore, we do not use IMDB in this section.

Figure 6 summarizes the results. First of all, the increasing number of parties will not decrease the performance of our attacks. For CIFAR10, the attacks’ performance even increases when there are more parties. We speculate it is because features are evenly distributed when the number of participants increases. Then, there will not exist a participant who can dominate the model’s predictions. In turn, it also means the adversary’s contribution to the top model is increasing, which makes v_{ae} easier to flip the prediction. The increased importance also makes it easier to strengthen the connection between the trigger and the target class. As shown in Figure 6, for CIFAR10, the poisoning attack’s performance improves when the number of parties increases.

However, for BANK, the poisoning attack’s performance first improves and drops when the number of parties is larger than 5. We speculate that the data type causes the difference. Specifically, when the number of parties increases, each party has fewer attributes. Since most attributes are discrete in BANK, fewer attributes mean fewer combinations of different values. Then, if one of these combinations, such as a white man living in Pennsylvania, happens to be frequently present in the dataset and is tied to a certain label, then it is very easy for the model to learn and rely on this pattern. This phenomenon is more likely to happen in a binary classification task than a multi-classes task, which may explain the difference between BANK and CIFAR10.

As for the fluctuation on both datasets, we speculate that it is caused by the randomness in the generation process, e.g., the randomness of coordinate selection. If the coordinates related to the target class are selected multiple times, its value will be optimized better, leading to a better attack performance.

6.2 Number of Classes

In this section, we evaluate our attacks when there is a larger number of classes. The purpose of this evaluation is to explore the impact of the number of classes on our attacks. As in previous

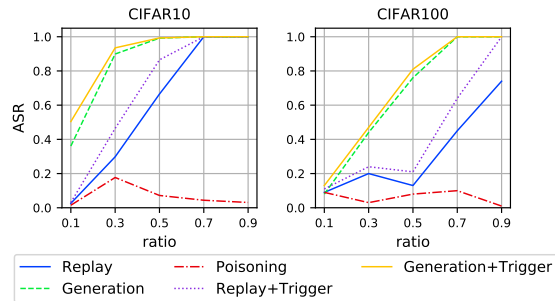


Figure 7: Attack performance when the number of classes changes. The x-axis denotes the ratio of features possessed by the adversary. The y-axis denotes the ASR of our attacks.

sections, we have mentioned that complex classification boundaries could make generating v_{ae} hard. Then to control the variables, we use CIFAR10 and CIFAR100 for evaluation. We conduct experiments with $\mathcal{K} = (\mathcal{P}, \mathcal{L}_{target})$, as the adversary can perform the most potent attack.

Figure 7 shows the results of these two datasets with different feature ratios. We have introduced the performance for CIFAR10 in Section 5.2, and we do not repeat it. The performance of our attacks on CIFAR100 drops as expected. Specifically, the replay attack can only achieve an ASR of 76% when the ratio is 90% of the total features, while for CIFAR10, it reaches 100% at the ratio of 70%. Similarly, the ASR of the generation attack with trigger reaches 100% until the ratio is 70% for CIFAR10, which is only 50% for CIFAR100. The performance drop of our generation attacks for CIFAR100, compared to CIFAR10, is over 40% when the ratio is lower than 50%. However, considering there are 100 classes, of which the random guess’s success rate is only 1%, we think the performance is acceptable.

In summary, the experiments in this section show our attacks may lose some performance as the number of classes increases. However, they still work when there are 100 classes.

6.3 Impact of Source Class

Our previous evaluation is conducted with a fixed source-target pair by default. Therefore, it is also essential to evaluate our attacks under different source-target pairs. Specifically, we use CIFAR10 to conduct the following experiments, as it can generate 90 pairs. However, considering that exchanging the source and the target class may produce similar performance, we finally choose to vary the source class and fix the target class as ‘1’ (which is ‘automobile’ in CIFAR10) for evaluation. Furthermore, since different source-target pairs have different degrees of difficulty, the number of optimization steps required for our attacks is also different. Therefore, we further evaluate the performance under 300 and 3,000 times of optimization steps for comparison. In addition, we still let the adversary has 10% of the total features.

Table 1 summarizes the results. From the results of 300 times, it is obvious that the attack’s performance is impressive for classes that are similar in reality. However, the attack’s ability is significantly reduced for classes that are not close. For example, when the source class is ‘truck’, our generation attacks’ performance can reach an ASR of over 95% even with the query budget at 300 times.

Table 1: Attack performance of different source classes and query budget. The target class is fixed as ‘1’ (automobile).

Source Class	Epochs: 300		Epochs:3000	
	Generation Attack	Generation Attack with Trigger	Generation Attack	Generation Attack with Trigger
Airplane	23.40%	57.00%	88.80%	94.60%
Bird	0.70%	3.00%	99.10%	99.20%
Cat	0.20%	0.40%	97.70%	99.40%
Deer	1.70%	12.40%	72.70%	85.30%
Dog	0.50%	13.00%	99.70%	99.70%
Frog	63.70%	64.80%	93.90%	94.90%
Horse	17.60%	25.40%	96.90%	98.10%
Ship	93.20%	94.30%	94.00%	94.90%
Truck	95.00%	97.10%	98.60%	98.60%

However, all attacks have failed for animals, like ‘cat’. Indeed, for a robust classifier, this phenomenon is expected. We speculate that in the training process of the classifier, a coarse-grained boundary is first determined to distinguish vehicles and animals, and then a fine-grained boundary, such as automobiles, trucks, ships, etc., is determined by continuously minimizing the loss. Therefore, for the ‘automobile’ and ‘truck’ pair, it is easy for ZOO to find the optimum perturbation. In contrast, the optimization path is complex for the ‘bird’ and ‘automobile’ pair.

However, this difference is almost eliminated when we expand the query budget. The generation attacks all achieve an ASR of over 94% (except for ‘deer’, which may be caused by randomness in optimization).

We do not discuss the other three attacks (i.e., poisoning attack, replay attack with/without trigger) in detail since their performance also follows the closeness of the source class to the target class. In addition, as we have analyzed in Section 5.2, these three attacks cannot reach a high ASR when the feature ratio is limited to 10%.

6.4 Impact of Poisoning Attack

As mentioned in Section 6.1, a powerful poisoning attack can make generating effective v_{ae} much easier. Therefore, this section evaluates the impact of the number of poisoned samples on our attacks. Intuitively, with more samples being poisoned, the performance of the poisoning attack will be improved, and at the same time, other attacks’ capability should also be enhanced.

We use CIFAR10 to conduct the following experiments. Furthermore, we investigate the connection between the poisoning attack and the generation attack with trigger under different background knowledge, i.e., $\mathcal{K} = (\mathcal{P}, \mathcal{L}_{target})$ and $\mathcal{K} = (\times, \mathcal{L}_{all})$. We vary the sampling ratio of poisoned samples from 1% to 10% of the total samples for comparison. The settings of different generation attacks are the same as those in Section 5.2 and Section 5.3.

Figure 8 shows the final results. First of all, with more poisoning samples, the poisoning attack can achieve better performance. For example, when the poison ratio is 9%, the performance reaches an ASR of 38%, far better than the ASR of nearly 10% at the poison ratio of 1%.

The impact of the improvement of the poisoning attack is directly reflected on the performance of the generation attack under the knowledge of $\mathcal{K} = (\times, \mathcal{L}_{all})$. We speculate that when the trigger r becomes stronger, the surrogate model will rely on it more. Therefore, it can learn a much more similar classification boundary as the top model. As for the generation attack under the knowledge of $\mathcal{K} = (\mathcal{P}, \mathcal{L}_{target})$, the performance change also follows the same trend, i.e., the ASR improves with the increase of the poison

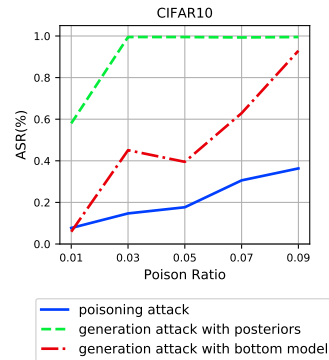


Figure 8: Poisoning effect comparison. The x-axis represents the ratio of poisoned samples to the total samples. The y-axis represents the ASR of attacks.

ratio. Moreover, this attack is much easier to achieve a high ASR with a further perturbed boundary. For example, when the poison ratio is 3% (nearly 150 samples), the ASR of generation attack with posteriors almost reaches 100%.

In conclusion, increasing the number of poisoned samples can not only improve the performance of the poisoning attack but also improve the performance of generation attacks when $\mathcal{K} = (\times, \mathcal{L}_{all})$ and $\mathcal{K} = (\mathcal{P}, \mathcal{L}_{all})$. This result also shows that if the performance of one attack is limited, e.g., generation attack under the knowledge of $\mathcal{K} = (\times, \mathcal{L}_{all})$, improving the other attack’s ability may help.

6.5 Additional Sensitivity Analysis

Analysis of the query budget on the generation attack. Our generation attack limits the query budget by 300 times. However, the generation attack is supposed to perform better when the query budget increases. Therefore, we further evaluate this factor’s impact. Due to the page limitation, we put the results in Appendix E.

Analysis of multi-modal’s impact on our attacks. VFL is a suitable framework for multi-modal learning. Therefore, we further analyze the impact of different modals on our attacks. We put the details in Appendix F due to the page limitation.

7 DEFENSE

7.1 Analysis of Existing Defense Methods

In this section, we mainly explore possible defense strategies against our attacks. Since we start a new track of attack against VFL, there is almost no existing dedicated defense research. Therefore, we look for possible defense methods on traditional models.

Specifically, since the adversary is a participant of VFL, the defense methods [23, 60, 78] with the assumption that there are a set of clean samples are not applicable. Then, for adversarial attacks, after excluding the detection methods, existing defense strategies focus on adversarial training [18, 64] and input transformation [24, 56]. Considering the adversarial training needs all participants to provide extra data, which means the adversary can still carry out the attack, we do not use this type of method as a defense. Moreover, adversarial training costs massive computation and communication sources, making it impractical in real business. Therefore, we adopt input transformation as one kind of defense method. Specifically,

following [56], in which the authors restricted the hidden space of DNNs, we normalize v_i from each participant for defense.

As for poisoning attacks, without being able to do data and model inspection offline, e.g., Neural Cleanse [78], the remaining works can be summarized as online detection, according to the classification in [19]. There are two popular streams in this category: Artificial Brain Stimulation (ABS) [45], which represents model inspection; and STRIP [20], which stands for data inspection. However, ABS needs to check the activation of neurons for detection, which violates the principle of data privacy and security of VFL. STRIP is based on the intuition that the posteriors of a sample added with strong perturbation, e.g., another sample belonging to other classes, should have high entropy. However, adding another sample’s features still needs the adversary’s collaboration, which is still not applicable. Furthermore, both methods still need to accumulate a set of samples’ normal ‘behavior’ after deployment to determine the threshold for identifying the abnormalities. Therefore, we cannot apply them for defense in VFL. Inspired by [29], which claimed that useful but non-robust features could cause misclassification, we speculate that our planted trigger also plays the same role that activates specific neurons to mislead the prediction results. Therefore, we introduce dropout [65] in the top model to reduce its memory of fixed features, especially those ‘polluted’ neurons. The following sections evaluate these two countermeasures against our attacks, i.e., normalization and dropout.

7.2 Normalization

In this section, we evaluate normalization’s impact on our attacks. Since we use ZOO to approximate gradients of a single coordinate, this strategy will seriously weaken our ability. We conduct experiments with the same setting as that in Section 5.2, where $\mathcal{K} = (P, \mathcal{L})$ and we vary the feature ratio of the adversary.

Figure 9 shows the results of our attacks’ performance under normalization. The impact is obvious on BANK and CIFAR10. For instance, when the feature ratio is 10%, our generation attack can only achieve an ASR of 50% on BANK, which is over 90% in Section 5.2. Furthermore, our attacks fail on CIFAR10 when the ratio is 10%, and the generation attack also drops from 92% to 53% when the ratio is 30%. For IMDB, however, this defense loses effect.

Despite the drop of performance on BANK and CIFAR10 at low feature ratios, our attacks’ performance remains when the feature ratio is over 50%. Moreover, for the binary classification task, where the other participant holds the remaining 90% of features, the ASR of nearly 50% is still a severe threat to real-world business.

7.3 Dropout

This section evaluates the defense effect of dropout. We add one dropout layer to the top model after the activation layer, e.g., ReLU. Then, we vary the probability of dropout from 0.1 to 0.9 for comparison. Here the probability denotes how likely a neuron’s value will be set to zero. Other settings are still the same as Section 5.2.

Figure 10 plots the results. For BANK, the performance of all attacks almost does not change with the increase of probability. However, the replay attack with trigger has been affected compared to that in Section 5.2, whose ASR drops from 40% to nearly 12%.

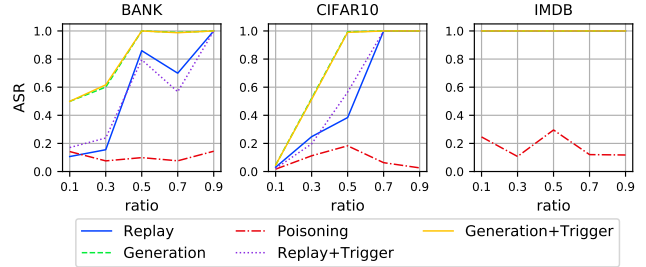


Figure 9: Attack performance using normalization. The x-axis denotes the ratio of features the adversary has. The y-axis denotes the ASR of our attacks.

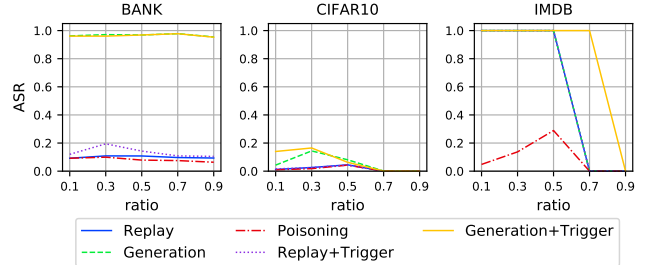


Figure 10: Attack performance when use dropout. The x-axis represents the set probability of dropout. The y-axis represents the ASR of attacks.

For CIFAR10, the performance of our attacks changes rapidly with the increase of the probability. When the probability is 10%, our attacks’ best ASR almost drops to 18%, and when the probability is over 50%, our attacks all fail. In order to figure out the reason why our attacks’ performance drops on CIFAR10, we further study the role of dropout. We find that as the probability increases from 10% to 90%, the accuracy of the classification task drops quickly from 78.04% to 18.56%. The low accuracy implies that the top model almost loses its ability to predict precisely. Therefore, our v_{ae} loses its effectiveness in flipping other samples’ predictions to the target class since the top model behaves like a random guess.

A similar phenomenon happens on IMDB. Specifically, except for the poisoning attack, other attacks keep the ASR of nearly 100% when the probability is under 50% but drop to 0 when the probability increases over 70%. We check the VFL model’s accuracy and find it is only 50% on the training dataset, which is a very poor performance (almost random guess) for binary classification.

In conclusion, the dropout can reduce the model’s memorization of specific patterns, which is helpful to defend against poisoning attacks. However, with a high probability of dropout, the main task’s performance also drops rapidly. This performance loss is unacceptable in practice.

8 RELATED WORK

8.1 Attacks and Defenses in FL

With FL becoming popular in industry, it is the new target of malicious attack and defense. However, the security and privacy of VFL are seldom studied yet. Therefore, we mainly introduce the attacks and defenses of HFL.

8.1.1 Attack Vectors. HFL deals with the case where participants have the same feature space \mathcal{F} but with different sample space \mathcal{U} . A standard application of HFL includes a global model at the server side and hundreds of local models at participants’ sides. Since the participant uses the model locally, studying the adversarial attack is trivial. Therefore, a line of works focuses on backdoor attacks against HFL. The backdoor attack against HFL aims to implement a backdoor in the global model. Therefore, an adversary can use the trigger to manipulate the results of the model users.

Bagdasaryan et al. first proposed the backdoor attack against HFL in [5]. They implemented a simple but effective way to inject a backdoor in the global model by scaling up the gradients. Then Sun et al. [69] further studied the backdoor attack’s efficacy in more complex scenarios, e.g., the EMNIST dataset, a real-life, user-partitioned, and non-iid dataset. Following [69], Wang et al. [80] further promoted the research of backdoor attack and claimed that the adversary could use samples from different distributions to make a stealthy attack, namely, attack of the tails. Xie et al. proposed an interesting idea in [87] which splits triggers into several parts and implement the attack in a distributed way.

In [46], Liu et al. first studied the backdoor attack against VFL. Specifically, they used the gradients of one sample belonging to the target class to replace the target samples. In this way, they avoided the limitation that the adversary cannot change labels in training. However, their experimental results show that their method is harmful to the original task’s performance and does not work on their selected datasets.

8.1.2 Defense Strategies. Corresponding to the attack vector mentioned above, we also investigate the existing defense strategies of HFL. The researches focus on detecting the updates from clients and the feedback from the global model.

Specifically, in [17], Fung et al. proposed a novel defense to this problem that identifies poisoning attacks based on the diversity of client updates in the distributed learning process. Compared to prior work, their system does not bound the expected number of adversaries and requires a fewer assumptions on clients and their data. Similarly, in [41], Li et al. proposed a new framework for robust federated learning where the central server learns to detect and remove the malicious model updates using a powerful detection model, leading to targeted defense. Different from checking the updates, in [4], Andreina et al. proposed a method to detect backdoor attacks via feedback-based federated learning (BAFFLE). The core idea behind BAFFLE is to leverage the data of multiple clients not only for training but also for uncovering model poisoning.

In addition, in [85], Wu et al. designed a federated pruning method to remove the redundant neurons in the network and then adjust the model’s extreme weight values.

8.2 Universal Adversarial Attacks

In [54], Moosavidez-Dezfooli et al. found the existence of a universal (image-agnostic) and small perturbation vector that causes natural images to be misclassified with high probability. However, the UAP generated by their method only aims to cause misclassification of the model without a target class. Therefore, it is not applicable for a malicious adversary who has the same goal in our work.

In [9], Brown et al. proposed a more powerful attack to create universal, robust, targeted adversarial image patches. Their evaluation results show that with careful design of the loss function, the generated adversarial patches can have an impressive attack performance. Similarly, in [21], Goh et al. found the neurons that are sensitive to specific features. Specifically, they showed that putting a card that printed ‘iPod’ on a Granny Smith apple would make their model misclassify it as iPod rather than an apple.

8.3 Remark

Our work is the first study of finding/generating an adversarial embedding to change the VFL model’s predictions. The goal of the backdoor attack against VFL proposed by Liu et al. [46] has overlapped with our work. However, their method only succeeds on MNIST [40], which is one of the two datasets listed in their work and is harmful to the original task’s performance. Our attacks perform impressively across all types of datasets. They can achieve the same goal even without the success of the poisoning attacks, and in the meantime, they do not harm the original task’s performance.

Pang et al. first analyzed the connection between adversarial and poisoning attacks in [59]. They claimed that combining backdoor attacks with adversarial perturbation can perform a more stealthy and efficient attack than using a single one. We also use the property of the two attack vectors to improve each other in our attack design. However, as mentioned in Section 1, we further solve the challenge of applying adversarial and poisoning attacks in VFL. Furthermore, the usage of the poisoning attack in our work is to address the challenge when the adversary only holds a few features.

9 DISCUSSION

9.1 Bypass Normalization

The evaluation of layer normalization’s impact on our attack shows it is an efficient way to defend black-box attacks like ZOO. The key to its success is to transform the perturbed input so that the adversary cannot approximate the gradients. Two possible attack strategies may solve the challenge. One is based on the perturbation’s transferability across models [61]. Another one can use the heuristic search for generating perturbations [7]. However, the surrogate model is hard to train in VFL because of the lack of $\{v_i\}_{i \neq adv}$.

In [7], Brendel et al. claimed that the generation of adversarial samples could also be implemented by heuristically search. A similar idea can also be seen in a line of works [73, 81]. We leave the exploration as our future work.

9.2 Integrated Defense

Evaluated defenses are proposed in traditional scenarios, mainly aiming at one specific attack. Our experimental results show that even if the defense prevents a part of our attack, e.g., the perturbation generation, it still cannot effectively defend against another part of the attack, i.e., the poisoning attack. This phenomenon reveals a new direction: we should design a defense considering both attack vectors, promising to provide more robust protection for DNNs based systems.

10 CONCLUSION

We present two specific attacks, i.e., replay attack and generation attack, to reveal VFL model's potential risks of being maliciously manipulated by one participant. The replay attack uses DNNs' sensitivity to signal patterns. The generation attack takes the joint force of adversarial and poisoning attacks to generate an optimal pattern, which can work when the adversary cannot modify labels and holds a few features. Furthermore, we investigate existing defense methods and evaluate two strategies against our attacks. Experimental results show our attacks' effectiveness and highlight the need for designing advanced defense strategies to protect VFL models.

REFERENCES

- [1] Ossama Abdel-Hamid, Abdel-rahman Mohamed, Hui Jiang, Li Deng, Gerald Penn, and Dong Yu. 2014. Convolutional neural networks for speech recognition. *IEEE/ACM Transactions on audio, speech, and language processing* 22, 10 (2014), 1533–1545.
- [2] Hagar Afriat, Shira Dvir-Gvirsman, Keren Tsuril, and Lidor Ivan. 2020. "This is capitalism. It is not illegal": Users' attitudes toward institutional privacy following the Cambridge Analytica scandal. *The Information Society* 37, 2 (2020), 115–127.
- [3] Scott Alfeld, Xiaojin Zhu, and Paul Barford. 2016. Data poisoning attacks against autoregressive models. In *Proceedings of the AAAI Conference on Artificial Intelligence*, Vol. 30.
- [4] Sebastien Andreina, Giorgia Azzurra Marson, Helen Möllering, and Ghassan Karame. 2021. Baffle: Backdoor detection via feedback-based federated learning. In *2021 IEEE 41st International Conference on Distributed Computing Systems (ICDCS)*. IEEE, 852–863.
- [5] Eugene Bagdasaryan, Andreas Veit, Yiqing Hua, Deborah Estrin, and Vitaly Shmatikov. 2020. How to backdoor federated learning. In *International Conference on Artificial Intelligence and Statistics*. PMLR, 2938–2948.
- [6] Dimitri P Bertsekas. 1997. Nonlinear programming. *Journal of the Operational Research Society* 48, 3 (1997), 334–334.
- [7] Wieland Brendel, Jonas Rauber, and Matthias Bethge. 2018. Decision-Based Adversarial Attacks: Reliable Attacks Against Black-Box Machine Learning Models. arXiv:1712.04248 [stat.ML]
- [8] Theodora S Brisimi, Ruidi Chen, Theofanie Mela, Alex Olshevsky, Ioannis Ch Paschalidis, and Wei Shi. 2018. Federated learning of predictive models from federated electronic health records. *International journal of medical informatics* 112 (2018), 59–67.
- [9] Tom B. Brown, Dandelion Mané, Aurko Roy, Martin Abadi, and Justin Gilmer. 2018. Adversarial Patch. arXiv:1712.09665 [cs.CV]
- [10] Nicholas Carlini and David Wagner. 2017. Towards evaluating the robustness of neural networks. In *2017 IEEE Symposium on Security and Privacy (SP)*. IEEE, 39–57.
- [11] Chaochao Chen, Jun Zhou, Li Wang, Xibin Wu, Wenjing Fang, Jin Tan, Lei Wang, Alex X Liu, Hao Wang, and Cheng Hong. 2021. When homomorphic encryption marries secret sharing: Secure large-scale sparse logistic regression and applications in risk control. In *Proceedings of the 27th ACM SIGKDD Conference on Knowledge Discovery & Data Mining*. 2652–2662.
- [12] Pin-Yu Chen, Huan Zhang, Yash Sharma, Jinfeng Yi, and Cho-Jui Hsieh. 2017. ZOO. *Proceedings of the 10th ACM Workshop on Artificial Intelligence and Security* (Nov 2017).
- [13] Yong Cheng, Yang Liu, Tianjian Chen, and Qiang Yang. 2020. Federated learning for privacy-preserving AI. *Commun. ACM* 63, 12 (2020), 33–36.
- [14] Jacob Devlin, Ming-Wei Chang, Kenton Lee, and Kristina Toutanova. 2019. BERT: Pre-training of Deep Bidirectional Transformers for Language Understanding. arXiv:1810.04805 [cs.CL]
- [15] Casey Fiesler, Nathan Beard, and Brian C Keegan. 2020. No robots, spiders, or scrapers: Legal and ethical regulation of data collection methods in social media terms of service. In *Proceedings of the international AAAI conference on web and social media*, Vol. 14. 187–196.
- [16] Chong Fu, Xuhong Zhang, Shouling Ji, Jinyin Chen, Jingzheng Wu, Shanqing Guo, Jun Zhou, Alex X. Liu, and Ting Wang. 2022. Label Inference Attacks Against Vertical Federated Learning. USENIX Association.
- [17] Clement Fung, Chris JM Yoon, and Ivan Beschastnikh. 2018. Mitigating sybils in federated learning poisoning. arXiv preprint arXiv:1808.04866 (2018).
- [18] Yaroslav Ganin, Evgeniya Ustinova, Hana Ajakan, Pascal Germain, Hugo Larochelle, François Laviolette, Mario Marchand, and Victor Lempitsky. 2016. Domain-adversarial training of neural networks. *The journal of machine learning research* 17, 1 (2016), 2096–2030.
- [19] Yansong Gao, Bao Gia Doan, Zhi Zhang, Siqi Ma, Jiliang Zhang, Anmin Fu, Surya Nepal, and Hyoungshick Kim. 2020. Backdoor attacks and countermeasures on deep learning: A comprehensive review. arXiv preprint arXiv:2007.10760 (2020).
- [20] Yansong Gao, Change Xu, Derui Wang, Shiping Chen, Damith C. Ranasinghe, and Surya Nepal. 2019. STRIP: A Defence against Trojan Attacks on Deep Neural Networks. In *Proceedings of the 35th Annual Computer Security Applications Conference (San Juan, Puerto Rico, USA) (ACSAC '19)*. Association for Computing Machinery, New York, NY, USA, 113–125. <https://doi.org/10.1145/3359789.3359790>
- [21] Gabriel Goh, Nick Cammarata †, Chelsea Voss †, Shan Carter, Michael Petrov, Ludwig Schubert, Alec Radford, and Chris Olah. 2021. Multimodal Neurons in Artificial Neural Networks. *Distill* (2021). <https://doi.org/10.23915/distill.00030> <https://distill.pub/2021/multimodal-neurons>.
- [22] Ian J Goodfellow, Jonathon Shlens, and Christian Szegedy. 2014. Explaining and harnessing adversarial examples. arXiv preprint arXiv:1412.6572 (2014).
- [23] Kathrin Grosse, Praveen Manoharan, Nicolas Papernot, Michael Backes, and Patrick McDaniel. 2017. On the (statistical) detection of adversarial examples. arXiv preprint arXiv:1702.06280 (2017).
- [24] Chuan Guo, Mayank Rana, Moustapha Cisse, and Laurens Van Der Maaten. 2017. Countering adversarial images using input transformations. arXiv preprint arXiv:1711.00117 (2017).
- [25] Andrew Hard, Kanishka Rao, Rajiv Mathews, Swaroop Ramaswamy, Françoise Beaufays, Sean Augenstein, Hubert Eichner, Chloé Kiddon, and Daniel Ramage. 2018. Federated Learning for Mobile Keyboard Prediction. arXiv:1811.03604 [cs.CL]
- [26] Kaiming He, Xiangyu Zhang, Shaoqing Ren, and Jian Sun. 2015. Deep Residual Learning for Image Recognition. arXiv:1512.03385 [cs.CV]
- [27] Febri Delis Herdiani. 2021. Analysis of Abuse and Fraud in the Legal and Illegal Online Loan Fintech Application Using the Hybrid Method. *Enrichment: Journal of Management* 11, 2 (2021), 486–490.
- [28] Andrew Ilyas, Logan Engstrom, Anish Athalye, and Jessy Lin. 2018. Black-box Adversarial Attacks with Limited Queries and Information. In *Proceedings of the 35th International Conference on Machine Learning (Proceedings of Machine Learning Research, Vol. 80)*, Jennifer Dy and Andreas Krause (Eds.). PMLR, 2137–2146. <https://proceedings.mlr.press/v80/ilyas18a.html>
- [29] Andrew Ilyas, Shibani Santurkar, Dimitris Tsipras, Logan Engstrom, Brandon Tran, and Aleksander Madry. 2019. Adversarial Examples Are Not Bugs, They Are Features. In *Advances in Neural Information Processing Systems*, H. Wallach, H. Larochelle, A. Beygelzimer, F. d'Alché-Buc, E. Fox, and R. Garnett (Eds.), Vol. 32. Curran Associates, Inc.
- [30] Leonardo H Iwaya, Simone Fischer-Hübner, Rose-Mharie Åhlfeldt, and Leonardo A Martucci. 2018. mhealth: A privacy threat analysis for public health surveillance systems. In *2018 IEEE 31st International Symposium on Computer-Based Medical Systems (CBMS)*. IEEE, 42–47.
- [31] Matthew Jagielski, Alina Oprea, Battista Biggio, Chang Liu, Cristina Nita-Rotaru, and Bo Li. 2018. Manipulating machine learning: Poisoning attacks and countermeasures for regression learning. In *2018 IEEE Symposium on Security and Privacy (SP)*. IEEE, 19–35.
- [32] Matthew Jagielski, Giorgio Severi, Niklas Pousette Harger, and Alina Oprea. 2020. Subpopulation data poisoning attacks. arXiv preprint arXiv:2006.14026 (2020).
- [33] Yujie Ji, Xinyang Zhang, Shouling Ji, Xiapu Luo, and Ting Wang. 2018. Model-reuse attacks on deep learning systems. In *Proceedings of the 2018 ACM SIGSAC conference on computer and communications security*. 349–363.
- [34] Bin Jiang, Jiachen Yang, and Houbing Song. 2020. Protecting privacy from aerial photography: State of the art, opportunities, and challenges. In *IEEE INFOCOM 2020-IEEE Conference on Computer Communications Workshops (INFOCOM WKSHPS)*. IEEE, 799–804.
- [35] Diederik P. Kingma and Jimmy Ba. 2017. Adam: A Method for Stochastic Optimization. arXiv:1412.6980 [cs.LG]
- [36] Daniel Kiselbach and Charles E Joern. 2012. New Consumer Product Safety Laws in Canada and the United States: Business on the Border. *Global Trade and Customs Journal* 7, 1 (2012).
- [37] Alex Krizhevsky, Geoffrey Hinton, et al. 2009. Learning multiple layers of features from tiny images. (2009).
- [38] Alex Krizhevsky, Ilya Sutskever, and Geoffrey E Hinton. 2012. Imagenet classification with deep convolutional neural networks. *Advances in neural information processing systems* 25 (2012), 1097–1105.
- [39] Peter D Lax and Maria Shea Terrell. 2014. *Calculus with applications*. Springer.
- [40] Yann LeCun, Léon Bottou, Yoshua Bengio, and Patrick Haffner. 1998. Gradient-based learning applied to document recognition. *Proc. IEEE* 86, 11 (1998), 2278–2324.
- [41] Suyi Li, Yong Cheng, Wei Wang, Yang Liu, and Tianjian Chen. 2020. Learning to detect malicious clients for robust federated learning. arXiv preprint arXiv:2002.00211 (2020).
- [42] Deron Liang, Chia-Chi Lu, Chih-Fong Tsai, and Guan-An Shih. 2016. Financial ratios and corporate governance indicators in bankruptcy prediction: A comprehensive study. *European Journal of Operational Research* 252, 2 (2016), 561–572. <https://doi.org/10.1016/j.ejor.2016.01.012>

- [43] Yang Liu, Tao Fan, Tianjian Chen, Qian Xu, and Qiang Yang. 2021. FATE: An Industrial Grade Platform for Collaborative Learning With Data Protection. *Journal of Machine Learning Research* 22, 226 (2021), 1–6. <http://jmlr.org/papers/v22/20-815.html>
- [44] Yang Liu, Yan Kang, Xinwei Zhang, Liping Li, Yong Cheng, Tianjian Chen, Mingyi Hong, and Qiang Yang. 2019. A communication efficient vertical federated learning framework. *arXiv preprint arXiv:1912.11187* (2019).
- [45] Yingqi Liu, Wen-Chuan Lee, Guan hong Tao, Shiqing Ma, Yousra Aafer, and Xiangyu Zhang. 2019. ABS: Scanning Neural Networks for Back-Doors by Artificial Brain Stimulation. In *Proceedings of the 2019 ACM SIGSAC Conference on Computer and Communications Security (London, United Kingdom) (CCS '19)*. Association for Computing Machinery, New York, NY, USA, 1265–1282. <https://doi.org/10.1145/3319535.3363216>
- [46] Yang Liu, Zhihao Yi, and Tianjian Chen. 2020. Backdoor attacks and defenses in feature-partitioned collaborative learning. *arXiv:2007.03608 [cs.LG]*
- [47] Xinjian Luo, Yuncheng Wu, Xiaokui Xiao, and Beng Chin Ooi. 2021. Feature Inference Attack on Model Predictions in Vertical Federated Learning. In *37th IEEE International Conference on Data Engineering, ICDE 2021, Chania, Greece, April 19-22, 2021*. IEEE, 181–192. <https://doi.org/10.1109/ICDE51399.2021.00023>
- [48] Lingjuan Lyu, Han Yu, Xingjun Ma, Lichao Sun, Jun Zhao, Qiang Yang, and Philip S Yu. 2020. Privacy and robustness in federated learning: Attacks and defenses. *arXiv preprint arXiv:2012.06337* (2020).
- [49] Andrew L. Maas, Raymond E. Daly, Peter T. Pham, Dan Huang, Andrew Y. Ng, and Christopher Potts. 2011. Learning Word Vectors for Sentiment Analysis. In *Proceedings of the 49th Annual Meeting of the Association for Computational Linguistics: Human Language Technologies*. Association for Computational Linguistics, Portland, Oregon, USA, 142–150. <http://www.aclweb.org/anthology/P11-1015>
- [50] James MacQueen et al. 1967. Some methods for classification and analysis of multivariate observations. In *Proceedings of the fifth Berkeley symposium on mathematical statistics and probability*, Vol. 1. Oakland, CA, USA, 281–297.
- [51] Aleksander Madry, Aleksandar Makelov, Ludwig Schmidt, Dimitris Tsipras, and Adrian Vladu. 2017. Towards deep learning models resistant to adversarial attacks. *arXiv preprint arXiv:1706.06083* (2017).
- [52] Arvind Mahindru. 2018. Android permission dataset. <https://doi.org/8y543xvnsv.1>
- [53] Luca Melis, Congzheng Song, Emiliano De Cristofaro, and Vitaly Shmatikov. 2019. Exploiting unintended feature leakage in collaborative learning. In *2019 IEEE Symposium on Security and Privacy (SP)*. IEEE, 691–706.
- [54] Seyed-Mohsen Moosavi-Dezfooli, Alhussein Fawzi, Omar Fawzi, and Pascal Frossard. 2017. Universal adversarial perturbations. *arXiv:1610.08401 [cs.CV]*
- [55] Seyed-Mohsen Moosavi-Dezfooli, Alhussein Fawzi, and Pascal Frossard. 2016. Deepfool: a simple and accurate method to fool deep neural networks. In *Proceedings of the IEEE conference on computer vision and pattern recognition*. 2574–2582.
- [56] Aamir Mustafa, Salman Khan, Munawar Hayat, Roland Goecke, Jianbing Shen, and Ling Shao. 2019. Adversarial defense by restricting the hidden space of deep neural networks. In *Proceedings of the IEEE/CVF International Conference on Computer Vision*. 3385–3394.
- [57] Milad Nasr, Reza Shokri, and Amir Houmansadr. 2019. Comprehensive Privacy Analysis of Deep Learning: Passive and Active White-box Inference Attacks against Centralized and Federated Learning. *2019 IEEE Symposium on Security and Privacy (SP)* (May 2019). <https://doi.org/10.1109/sp.2019.00065>
- [58] Xiang Ni, Xiaolong Xu, Lingjuan Lyu, Changhua Meng, and Weiqiang Wang. 2021. A Vertical Federated Learning Framework for Graph Convolutional Network. *arXiv:2106.11593 [cs.LG]*
- [59] Ren Pang, Hua Shen, Xinyang Zhang, Shouling Ji, Yevgeniy Vorobeychik, Xipu Luo, Alex Liu, and Ting Wang. 2020. A Tale of Evil Twins: Adversarial Inputs versus Poisoned Models. In *Proceedings of the 2020 ACM SIGSAC Conference on Computer and Communications Security (Virtual Event, USA) (CCS '20)*. Association for Computing Machinery, New York, NY, USA, 85–99. <https://doi.org/10.1145/3372297.3417253>
- [60] Tianyu Pang, Chao Du, Yinpeng Dong, and Jun Zhu. 2018. Towards Robust Detection of Adversarial Examples. In *Advances in Neural Information Processing Systems*, S. Bengio, H. Wallach, H. Larochelle, K. Grauman, N. Cesa-Bianchi, and R. Garnett (Eds.), Vol. 31. Curran Associates, Inc.
- [61] Nicolas Papernot, Patrick McDaniel, and Ian Goodfellow. 2016. Transferability in Machine Learning: from Phenomena to Black-Box Attacks using Adversarial Samples. *arXiv:1605.07277 [cs.CR]*
- [62] Debidutta Pattnaik, Mohammad Kabir Hassan, Satish Kumar, and Justin Paul. 2020. Trade credit research before and after the global financial crisis of 2008 – A bibliometric overview. 54 (dec 2020), 101287. <https://doi.org/10.1016/j.ribaf.2020.101287>
- [63] Ali Shafahi, W. Ronny Huang, Mahyar Najibi, Octavian Suci, Christoph Studer, Tudor Dumitras, and Tom Goldstein. 2018. Poison Frogs! Targeted Clean-Label Poisoning Attacks on Neural Networks. In *Proceedings of the 32nd International Conference on Neural Information Processing Systems (Montréal, Canada) (NIPS'18)*. Curran Associates Inc., Red Hook, NY, USA, 6106–6116.
- [64] Ali Shafahi, Mahyar Najibi, Amin Ghiasi, Zheng Xu, John Dickerson, Christoph Studer, Larry S Davis, Gavin Taylor, and Tom Goldstein. 2019. Adversarial training for free! *arXiv preprint arXiv:1904.12843* (2019).
- [65] Nitish Srivastava, Geoffrey Hinton, Alex Krizhevsky, Ilya Sutskever, and Ruslan Salakhutdinov. 2014. Dropout: A Simple Way to Prevent Neural Networks from Overfitting. *J. Mach. Learn. Res.* 15, 1 (Jan. 2014), 1929–1958.
- [66] Emma Strubell, Ananya Ganesh, and Andrew McCallum. 2019. Energy and policy considerations for deep learning in NLP. *arXiv preprint arXiv:1906.02243* (2019).
- [67] Jiawei Su, Danilo Vasconcellos Vargas, and Kouichi Sakurai. 2019. One Pixel Attack for Fooling Deep Neural Networks. *IEEE Transactions on Evolutionary Computation* 23, 5 (oct 2019), 828–841. <https://doi.org/10.1109/tevc.2019.2890858>
- [68] Octavian Suci, Radu Marginean, Yigitcan Kaya, Hal Daume III, and Tudor Dumitras. 2018. When does machine learning {FAIL}? generalized transferability for evasion and poisoning attacks. In *27th {USENIX} Security Symposium ({USENIX} Security 18)*. 1299–1316.
- [69] Ziteng Sun, Peter Kairouz, Ananda Theertha Suresh, and H Brendan McMahan. 2019. Can you really backdoor federated learning? *arXiv preprint arXiv:1911.07963* (2019).
- [70] Fnu Suya, Jianfeng Chi, David Evans, and Yuan Tian. 2020. Hybrid Batch Attacks: Finding black-box adversarial examples with limited queries. In *USENIX Security Symposium*.
- [71] Christian Szegedy, Alexander Toshev, and Dumitru Erhan. 2013. Deep neural networks for object detection. (2013).
- [72] Ruixiang Tang, Mengnan Du, Ninghao Liu, Fan Yang, and Xia Hu. 2020. An embarrassingly simple approach for trojan attack in deep neural networks. In *Proceedings of the 26th ACM SIGKDD International Conference on Knowledge Discovery & Data Mining*. 218–228.
- [73] Rohan Taori, Amog Kamsetty, Brenton Chu, and Nikita Vemuri. 2019. Targeted adversarial examples for black box audio systems. In *2019 IEEE Security and Privacy Workshops (SPW)*. IEEE, 15–20.
- [74] Ian Tenney, Dipanjan Das, and Ellie Pavlick. 2019. BERT rediscovers the classical NLP pipeline. *arXiv preprint arXiv:1905.05950* (2019).
- [75] Alexander Turner, Dimitris Tsipras, and Aleksander Madry. 2019. Clean-Label Backdoor Attacks. <https://openreview.net/forum?id=HJg6e2CkK7>
- [76] L. G. Valiant. 1984. A Theory of the Learnable. *Commun. ACM* 27, 11 (nov 1984), 1134–1142. <https://doi.org/10.1145/1968.1972>
- [77] Paul Voigt and Axel Von dem Bussche. 2017. The EU general data protection regulation (gdpr). *A Practical Guide, 1st Ed., Cham: Springer International Publishing* (2017).
- [78] Bolun Wang, Yuanshun Yao, Shawn Shan, Huiying Li, Bimal Viswanath, Haitao Zheng, and Ben Y Zhao. 2019. Neural cleanse: Identifying and mitigating backdoor attacks in neural networks. In *2019 IEEE Symposium on Security and Privacy (SP)*. IEEE, 707–723.
- [79] Guan Wang. 2019. Interpret Federated Learning with Shapley Values. <https://doi.org/10.48550/ARXIV.1905.04519>
- [80] Hongyi Wang, Kartik Sreenivasan, Shashank Rajput, Harit Vishwakarma, Saurabh Agarwal, Jy-yong Sohn, Kangwook Lee, and Dimitris Papailiopoulos. 2020. Attack of the tails: Yes, you really can backdoor federated learning. *arXiv preprint arXiv:2007.05084* (2020).
- [81] Lina Wang, Kang Yang, Wenqi Wang, Run Wang, and Aoshuang Ye. 2020. MGAAttack: Toward More Query-efficient Black-box Attack by Microbial Genetic Algorithm. In *Proceedings of the 28th ACM International Conference on Multimedia*. 2229–2236.
- [82] Webank. 2020. A case of traffic violations insurance-using federated learning. <https://www.fedai.org/cases>.
- [83] Webank. 2020. Utilization of FATE in Risk Management of Credit in Small and Micro Enterprises. <https://www.fedai.org/cases>.
- [84] Haiqin Weng, Juntao Zhang, Feng Xue, Tao Wei, Shouling Ji, and Zhiyuan Zong. 2021. Privacy Leakage of Real-World Vertical Federated Learning. *arXiv:2011.09290 [cs.CR]*
- [85] Chen Wu, Xian Yang, Sencun Zhu, and Prasenjit Mitra. 2021. Mitigating Backdoor Attacks in Federated Learning. *arXiv:2011.01767 [cs.CR]*
- [86] Huang Xiao, Battista Biggio, Gavin Brown, Giorgio Fumera, Claudia Eckert, and Fabio Roli. 2015. Is feature selection secure against training data poisoning?. In *international conference on machine learning*. PMLR, 1689–1698.
- [87] Chulin Xie, Keli Huang, Pin-Yu Chen, and Bo Li. 2019. Dba: Distributed backdoor attacks against federated learning. In *International Conference on Learning Representations*.
- [88] Jie Xu, Benjamin S. Glicksberg, Chang Su, Peter Walker, Jiang Bian, and Fei Wang. 2020. Federated Learning for Healthcare Informatics. *arXiv:1911.06270 [cs.LG]*
- [89] Qiang Yang, Yang Liu, Tianjian Chen, and Yongxin Tong. 2019. Federated machine learning: Concept and applications. *ACM Transactions on Intelligent Systems and Technology (TIST)* 10, 2 (2019), 1–19.
- [90] Hongyi Zhang, Moustapha Cisse, Yann N. Dauphin, and David Lopez-Paz. 2018. mixup: Beyond Empirical Risk Minimization. *arXiv:1710.09412 [cs.LG]*

- [91] Jun Zhou, Chaochao Chen, Longfei Zheng, Huiwen Wu, Jia Wu, Xiaolin Zheng, Bingzhe Wu, Ziqi Liu, and Li Wang. 2021. Vertically Federated Graph Neural Network for Privacy-Preserving Node Classification. arXiv:2005.11903 [cs.LG]
- [92] Ligeng Zhu, Zhijian Liu, and Song Han. 2019. Deep leakage from gradients. In *Advances in Neural Information Processing Systems*. 14774–14784.
- [93] Yushan Zhu, Xing Tong, and Xi Wang. 2019. Identifying privacy leakage from user-generated content in an online health community—a deep learning approach. In *2019 IEEE International Conference on Healthcare Informatics (ICHI)*. IEEE, 1–2.

A SYMBOLS AND NOTATIONS

Table 2 summarizes the important notations in the paper.

Table 2: Symbols and notations.

Notations	Definition
m	the number of participants
P_i	the i -th participant
D_i, U_i, F_i	P_i 's dataset, D_i 's sample space, D_i 's feature space
f_i, f_{top}, f_s	P_i 's bottom model, the top model, the surrogate model
$\theta_i, \theta_{top}/\theta_{m+1}$	f_i 's parameters, f_{top} 's parameters
x_i^u, v_i^u	sample u 's feature vector from D_i , x_i^u 's output from f_i
d_i, d_*	size of F_i , size of bottom models' output
n_c	number of classes
c, t, s	class c , target class, source class
δ, δ_*	adversarial perturbation, optimal perturbation
θ_δ, θ_*	perturbed parameters, optimal perturbed parameters

B DETAILS OF DERIVATION

We introduce the ZOO method to solve Eq 4 as follows. Since $\{v_i\}_{i \neq adv}$ and $\{\theta_i\}_{i \neq adv}$ are fixed, we take them as unknown parameters. Then, we use F to denote the function that calculates the posteriors based on v_{adv} , i.e., $F(v_{adv}; \{v_i\}_{i \neq adv}, \{\theta_i\}_{i \neq adv})$. Then, the loss function of Eq 4 can be reformulated as

$$\ell(\delta) = \max \left\{ F(\delta)_t - \max_{i \neq t} (F(\delta)_i), -\kappa \right\},$$

where $\kappa \geq 0$ is a constant. The new loss function expands the gap between class t 's posterior and the maximum posterior except t . Note that t 's posterior may not be the maximum at first, and κ is then used to clip the loss. Then, Eq 4 can be represented as

$$v_{ae} = \max_{\delta \in \mathbb{R}^{d_*}} \{\ell(\delta)\}.$$

To optimize the new objective function, we use the symmetric difference quotient [39] to estimate the gradient $\frac{\partial \ell(\delta)}{\partial \delta_i}$ (defined as \hat{g}_i):

$$\hat{g}_i := \frac{\partial \ell(\delta)}{\partial \delta_i} \simeq \frac{\ell(\delta + h e_i) - \ell(\delta - h e_i)}{2h} \quad (7)$$

where h is a constant and e_i is a standard base vector with only the i -th component as 1. With the coordinate-related gradient, the following optimization process is completed by the coordinate descent method [6], which randomly chooses the coordinate and repeats the optimization until the objective function is satisfied. Furthermore, to achieve stable performance, we use momentum in our optimization like Adam [35]. The implementation follows Chen et al. in [12].

C DETAILS OF IMPLEMENTATION

In our implementation, there are several default settings. We summarize them as follows.

Table 3: Default parameter setting for models.

Model/Optimizer	Parameter	Setting
DNNs for the bottom model	size of hidden layer	$n = 64$
	size of output dimension	$n = 16$
DNNs for the top model	size of hidden layer	$n = 64$
	size of input layer	$n = 16 \times m$
	number of block layers	$n = 18$
ResNet	size of output dimension	$n = 16$
BERT	type	bert-base-uncased
Surrogate model	number of fully connected layers	$n = 1$
	size of input layer	$n = 16$
Adam	learning rate	$lr = 0.01$
	weight decay	$wd = 0.0001$
VFL	training epoch	$epochs = 10$
	batch_size	$bs = 256$ by default, $bs = 8$ for NLP

Table 4: Default parameter setting for attacks.

Attack	Parameter	Setting
Clean-label Attack	time to poison samples	$epoch = 5$
	poison ratio	1%, e.g., 50 for CIFAR10
ZOO-Adam	optimization steps	$n_{iter} = 300$
	height	$h = 0.01$
	step	$step = 0.1$
	gradient factor	$\beta_1 = 0.9$
	momentum factor	$\beta_2 = 0.999$
Mix-up	training epoch	$epoch = 100$
	random seed	$\alpha = 1$

C.1 Parameter Setting for Models

Table 3 summarizes the default parameter setting in our empirical evaluations.

C.2 Parameter Setting for Attacks

The classes are encoded as numbers. By default, we set the source class as '0' and the target class as '1'. Table 4 summarizes the default parameter setting for our attacks.

D ALGORITHMS

D.1 Algorithm of Generation Attack When

$$\mathcal{K} = (\mathcal{P}, \mathcal{L}_{target})$$

Algorithm 2 summarizes the process of the attack when $\mathcal{K} = (\mathcal{P}, \mathcal{L}_{target})$.

Algorithm 2 Adversarial Embedding Generation with Poisoning Attack

Require: Auxiliary set of samples with target label \mathcal{L}_{target} ; samples who have high confidence of the source class \mathcal{S} ; query budget Q .

Ensure: Adversarial embedding v_{ae} .

- 1: Generate Gaussian noise r .
- 2: Add r on embeddings from \mathcal{L}_{target} , and upload them in training.
- 3: $\delta \leftarrow r$, $queries \leftarrow 0$
- 4: **for** $s \in \mathcal{S}$ **do**
- 5: **while** $queries < \frac{Q}{|\mathcal{S}|}$ **do**
- 6: randomly choose coordinate i
- 7: $\hat{g}_i \leftarrow \text{ZOO-Adam}(\ell([v_1, \dots, \delta, \dots, v_m]^s, t))$
- 8: $\delta_i \leftarrow \delta_i - \hat{g}_i$
- 9: $queries \leftarrow queries + 2$
- 10: **end while**
- 11: $queries \leftarrow 0$
- 12: **end for**
- 13: $v_{ae} \leftarrow \delta$

D.2 Algorithm of Generation Attack When

$$\mathcal{K} = (\mathcal{X}, \mathcal{L}_{all})$$

Algorithm 3 summarizes the process of the attack when $\mathcal{K} = (\mathcal{X}, \mathcal{L}_{all})$.

Algorithm 3 Adversarial Embedding Generation with Auxiliary Dataset

Require: Auxiliary set of samples with all classes \mathcal{L}_{all} , threshold ϵ .

Ensure: Adversarial embedding v_{ae} .

- 1: Generate Gaussian noise r .
 - 2: Add r on embeddings of samples with target label from \mathcal{L}_{all} , and upload them at training time.
 - 3: Using Mix-up to train a surrogate model f_s .
 - 4: Collecting a sample u with high confidence of target class through f_s .
 - 5: $\delta \leftarrow v_{adv}^u + r$, error bound ϵ .
 - 6: **while** $\ell(f_s(\delta), t) > \epsilon$ **do**
 - 7: $\delta \leftarrow \delta - \frac{\partial \ell(f_s(\delta), t)}{\partial \delta}$
 - 8: **end while**
 - 9: $v_{ae} \leftarrow \delta$
-

E NUMBER OF QUERIES

The experiments conducted in this section reveal the impact of the query budget on our attacks. We use the generation attack for evaluation and vary the number of queries from 300 to 3,000. We still use BANK and CIFAR10 in this evaluation.

Figure 11 shows the results of the generation attack’s performance with different query budgets. For different datasets, the change of the performance seems to show two different trends. Specifically, for BANK, the generation attack can achieve an ASR of almost 91% with only 300 queries. Then, with the increase of the query budget, the performance drops and then remains at 80%. However, for CIFAR10, the performance increases with the number of queries increasing.

We speculate that the number of classes causes the difference. For the binary classification task, like BANK, it is easy to find a way to cross the classification boundary. Then, according to our attack design, with more queries, the generated perturbation may overfit the collected samples of the source class, which reduces its performance on test samples. For the multi-class task, like CIFAR10, things are different. The classification boundary is much more complex than the binary case. Therefore, the generation attack takes around 2,100 queries to achieve an ASR of over 80% on CIFAR10 than BANK. Indeed, when the number of queries is larger than 2,700, the ASR on CIFAR10 also drops slightly.

In conclusion, the performance of the generation attack will increase as the number of queries increases at the beginning. However, when the number of optimization steps exceeds the task’s difficulty, it may lead to overfitting, which causes a certain loss in the attack’s performance. It suggests that when implementing our attack in practice, the adversary should check the attack’s performance after empirical rounds of optimization and stop the process to avoid the loss of the attack’s efficiency.

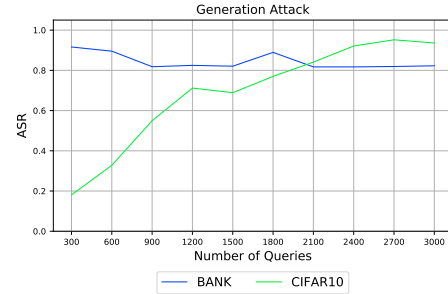


Figure 11: The generation attack’s performance with different query budgets. The x-axis represents the number of queries. The y-axis represents the ASR of attacks.

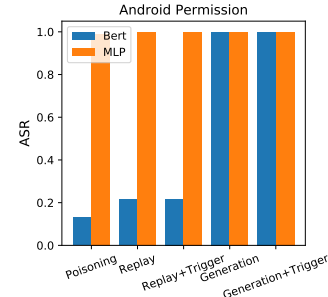


Figure 12: Comparison of attack performance between two modal data.

F IMPACT OF MODALS

The characteristics of VFL make it a very suitable framework for multi-modal learning. Therefore, in this section, we mainly evaluate the attacks in a multi-modal scenario. Specifically, we use AP to conduct the experiments and evaluate our attacks with $\mathcal{K} = (\mathcal{P}, \mathcal{L}_{target})$. In AP, text data and tabular data are included. The text data is the description of an APP. The tabular data counts the characteristics of an APP, such as the number of permissions and the security level of these requested permissions. Intuitively, the importance of the tabular data is much higher than the text data. Therefore, the attacks at the tabular data side are supposed to perform better than those on the text data.

Figure 12 plots the results. When the adversary owns the tabular data, it is impressive that for all attacks, the ASR reaches 100%. However, for text data, only our generation attacks can achieve the same performance. As for the backdoor attack and replay attacks, the importance of the text data for classification is limited, e.g., their performance is around 20%. This fact verifies our speculation that a participant with more important data for the top model can carry out a more threatening attack.

In conclusion, our attacks are modal agnostic since the adversary controls the bottom model. Furthermore, the importance of the data for the task determines the attack’s ability.